Helium and Heat Correlation

x-ray, heat excess and ^{4}He in the electrochemical confinement of deuterium in palladium

F. Cellucci[#] P.L. Cignini[#], G. Gigli, D. Gozzi[&], M. Tomellini[*]
Dipartimento di Chimica, Università di Roma La Sapienza, P.le Aldo Moro 5, 00185 Roma, Italy

E. Cisbani[§], S. Frullani, F. Garibaldi, M. Jodice[§], G.M. Urciuoli[§]
Laboratorio di Fisica, Istituto Superiore di Sanità, V.le Regina Margherita 299, 00161 Roma, Italy

Abstract
The energy balance between heat excess and ^{4}He in the gas phase has been found reasonably satisfied even if the low levels of ^{4}He found do not give the necessary confidence to state definitely that we are dealing with the fusion of deuterons to give ^{4}He. In the melted cathode, whose data are reported here, ^{4}He was not found at the achieved sensitivity. X-ray film, positioned at 50 mm from the cell, roughly gave the image of the cathode through spots. The energy of the radiation and the total energy associated to it have been, respectively, evaluated as (89±1) keV and (12.0 ± 0.4) kJ. This value is ≈ 0.5% of the energy measured by calorimetry in the same interval of time.

1. Introduction

The debate on the anomalous behaviour of the system Pd-D is still open because, in spite of the intense research activity lasted seven years in several laboratories worldwide, a clear-cut picture of all the evidences claimed is still lacking. Since 1989[1], many papers have been published, six international conferences were held on this subject, several patents issued, some promising theory has been proposed but, from an experimental point of view, the crucial initial point, the energy balance, has not yet found a satisfactorily and convincing explanation. All the efforts done to explain the excess heat found as of chemical nature have been so far considered meaningless because no chemical reaction we can imagine in the environment where the experiments of deuterium confinement generally occur is suitable to get comparable amounts of heat. The whole situation, restricted only to the heat excess findings, easily brings to the following consideration: either heat excess measurements are all experimental artifacts or we are dealing with new phenomena. By examining the abundant literature and some critical revisions[2,3] as well as through our direct experience gained in the field[4-6], there are not so strong evidences to believe that we are in the presence of a collective world-wide mistake in measuring the heat excess. Several laboratories, using different techniques and protocols found the same phenomenology and comparable results even if the reproducibility and a full control of the experiments are still lacking. On the other hand, many experiments show other phenomena associated to the heat excess production the source of which does not seem reasonably to be based on the Chemistry: emission of x-ray[7-9], as it will be shown in this paper, and neutrons[10-13] as well as production of ^{4}He[14-17] and ^{3}H[6,18-21]. Unfortunately, the intensities and the levels of these emissions and productions are so low that their detection is sometimes very critical and difficult to accept as statistically significative

CNR-Centro di Termodinamica Chimica Alle Alte Temperature, c/o Dipartimento di Chimica, Università di Roma *La Sapienza*, P.le Aldo Moro 5, 00185 Roma, Italy
&To whom correspondence should be addressed
* Dipartimento di Scienze e Tecnologie Chimiche, Università di Roma *Tor Vergata*, Via della Ricerca Scientifica, 00133 Roma, Italy
§ National Instiute for Nuclear Physics, sez. Sanità, Laboratorio di Fisica, Istituto Superiore di Sanità, V.le Regina Margherita 299, 00161 Roma, Italy

results. Though, for the above reasons, the reliability of such no calorimetric evidences is often poor, the whole picture seems to be very intriguing so that it cannot be shortly ruled out defining it as an *ensemble* of mistakes and artifacts. Can a simple physico-chemical process, like the insertion of deuterium into the Pd lattice, whose energy is ≈ 0.1 eV/cm^3, get x-ray emission or other nuclear products at tenths of keV or some MeV? The answer is not based on the Chemistry we know but the answer seems hard to find also in the current knowledges of Physics. Quite-zero energy of the particles in the solid state, the Coulomb barrier, very low cross-sections of possible nuclear reactions, etc. are very strong arguments to consolidate skepticism and criticism. The scope of this work, based on the electrochemical confinement of deuterium in palladium, is to report and discuss the experimental facts we found in the last experiment which was the most complex and complete among the experiments we did since 1989.

2. Experimental

A detailed description of the entire experimental set-up is given elsewhere[5,6]. Here it will be described the new features added or modified with respect to the past published work.

2.1 Electrochemical & calorimetric cell

It is a Pyrex-stainless steel cell designed to accomplish the following tasks: *i)* to avoid any ^{4}He contamination (^{4}He content in air is 5.24 ppm) of the escaping electrolysis gases in which ^{4}He is to be on line measured. This is obtained by a high-vacuum tested SS holder containing the part of the cell emerging from the thermostatic bath. A stream of ^{4}He free boiling-off LN_2 circulates inside and outside the cell at 35 sccm and 2.25 Bar ; *ii)* to be a flow-calorimeter in which the circulating water can exchange heat only with the electrolytic solution. This is realized by two jackets external to the pyrex tube containing the electrolyte solution. The innermost jacket is used for the circulation of double distillated water at constant flow-rate and the outermost one is sealed under high vacuum and it is mirror-like on the top to minimize the leakage of heat by radiation; *iii)* to maintain constant the level of the electrolyte through an optoelectronic sensor controlling the feed of D_2O which is consumed during the experiment by the electrolysis, according to the Faraday's law, and evaporation; *iv)* to perform *in situ* heat calibrations through an internal resistor. At the stationary state, the energy balance of the cell is given by the equation below as:

$$P_{in} + P_{cal} + P_{exc} = P_w + P_{rad} + P_{sg} \qquad (1)$$

where the subscripts *in*, *cal*, *exc*, *w*, *rad* and *sg* stand, respectively, for the input through the electric power applied to carry out the electrolysis, power through the internal heater for making in situ calibrations, power in excess to be measured, power exchanged by the water stream crossing the innermost jacket, power radiated from the cell toward the bath and the power necessary to saturate with D_2O vapor the gas stream which is composed by the protective gas N_2 and electrolysis gases D_2 and O_2. Its composition, at fixed N_2 flow-rate, q_{N_2}, depends on the electrolysis current I. At t > τ, the time constant of the cell, eqn. 2 below, through eqn. 1, would allow to calculate P_{exc} [6]:

$$P_{exc} + V_h I_h + (V_{in} - V_{th})I = (\rho c_l q)_{H_2O}\Delta\vartheta_{wj,\infty} + \\ + k_{Rad}S_s\left\{\left[\vartheta_{tb} + \Delta\vartheta_{wj,\infty}\right]^4 - \vartheta_{tb}^4\right\} + \qquad (2) \\ + \left(\frac{3I}{4F} + \frac{P}{R\vartheta_r}q_{N_2}\right)\left[\frac{p(\vartheta_s)}{P - p(\vartheta_s)}\right]\left[\left(C_g - C_l\right)_{D_2O}\vartheta_s + \Lambda_{D_2O}\right]$$

Equation 2 can be used provided the temperature difference, $\Delta\vartheta_{wj,\infty}$, at inlet and outlet of water cooled jacket, the temperature of the bath, ϑ_{tb}, the cooling water flow-rate, q, the potential drop, V_{in}(I), at the electrodes, the room temperature, ϑ_r, the temperature of the solution, ϑ_s, and the total pressure P are measured during the experiment. $p(\vartheta_s)$ is the vapor pressure of the solution at temperature ϑ_s. Λ_{D_2O}, C_g and C_l are quantities referred to D_2O, respectively, the heat of evaporation, heat capacity of gas and liquid. V_{th} is the thermoneutral potential (1.5367 V)[22] for the

decomposition of D_2O and the product $V_h I_h$ is the input power applied to the internal resistor when the calibration step is on. S_s is the radiating surface area of the cell and k_{Rad} the Stefan-Boltzmann constant. However, instead of using eqn. 2, it is common practice to perform the calibration of the cell both before starting the electrolysis and in progress by making use of the internal heater in both the cases. Figure 1 shows the typical response of a blank cell (Pt cathode implies that $P_{exc} = 0$) when step-fashion variations of the input power (right scale) are applied to it. In this case, we have superimposition of power generated by the internal heater and a constant thermal power generated by electrolysis. The stationary values of $\Delta\vartheta_{wj,\infty}$ *vs* the input power represent the calibration. The different slopes are connected to the different flow-rates of water in the cooling jacket as reported in Table I. The straight-line behaviour of the calibration curves shows that the 2nd and 3rd term of the right side of eqn. 2 are either negligible or their sum is linear too. This is in fact what one finds by an estimation of the terms P_{rad} and P_{sg} assuming[6]: I= 1A, S_s = 240 cm^2, ϑ_{tb}= 21 °C, ϑ_f = 30 °C, q_{N_2} = 5.8x10^{-7} m^{3}s^{-1} and P=2.25 Bar as typical values. The time constant of the cell is a function of the cooling water flow-rate and, for example, its value in the conditions of Fig. 1 is 270 s. By increasing the flow-rate the time constant decreases but this makes the sensitivity (the slope of the calibration curve) poor.

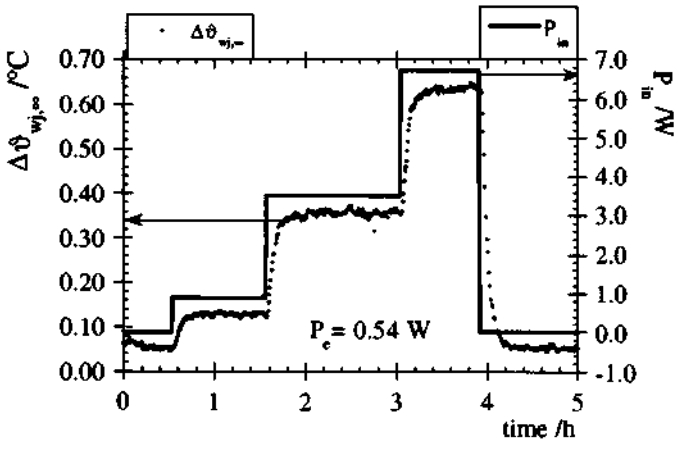

Fig. 1. Response of the cell at step variations of input power generated by the internal heater while electrolysis is running.

Table I.

Calibration curves given by the best fitting equations $\Delta\vartheta_{wj,\infty} = (a \pm \Delta a) + (b \pm \Delta b)\, P_{in}$.

The flow-rates in brackets are the expected values.

Cell #	(a ± Δa)/°C	(b± Δb) /°CW^{-1}	R	flow-rate/cm^{3}s^{-1}
1(blank)	0.02±0.01	0.118±0.001	0.99944	1.9 (2.03)
2	0.00±0.03	0.104±0.002	0.99736	2.1 (2.31)
3	-0.09±0.04	0.144±0.003	0.99738	1.5 (1.67)
4	-0.048±0.009	0.0871±0.0007	0.99965	2.5 (2.75)

Electrodes

All the anodes were made of pure platinum from Engelhard and shaped as gauze cylinders having the skeleton made of 1 mm dia. wires supporting the spot-welded mesh made of 0.35 mm dia. wire. The mesh dimension was 5x4 mm^2 and the anode final size was 48 mm height and 12 mm inner diameter. All the cathodes, except the cathode of the blank cell, were made of pure palladium from Engelhard and shaped as bundle of wires wrapped at the ends by machined cylindrical pieces of 6 mm Pd rods.The overall external dimensions of the cathodes were 6 mm dia. x 55 mm height. The height of the bundle was 40 mm (only 24 mm were out of the wrapping) and its diameter about 4 mm. Two out of three cathodes were constituted by bundles of 150 wires of 250 μm dia. each and the other one by 42 wires of 500 μm. The cathode of the blank cell was shaped similarly but the bundle was realized by 10 Pt wires of 1 mm dia. and wrapped by using SS machined caps. All the cathodes were annealed in high vacuum at 970 °C for 24 hours and cooled at room temperature at a rate of 1 °C/min. This procedure greatly reduces internal stresses and dislocation concentration and it allows the growth of large grains as it was shown by the metallographic analysis which gave a distribution of 2D grain size centered at 35±5 μm (≈ 53 μm in 3D)[23].

2.3 X-ray detection

X-ray films (Kodak, type TM H/RA-1 18x24 cm^2) were used to detect emission from the cells. Before use the film was inserted in a plastic black bag in dark room and put in front of the cell 5 cm distant as reported in figure 2. It is important to point out that the films were not in direct contact

Fig. 2. Scheme of the X-ray positioning in the experimental set-up. R_t=250 mm is the radius of torus containing the cells (see fig. 8 of ref.6). d=50 mm and f=6.5 mm. The materials in between the cell and film are H2O (45 mm) and perspex (5 mm).

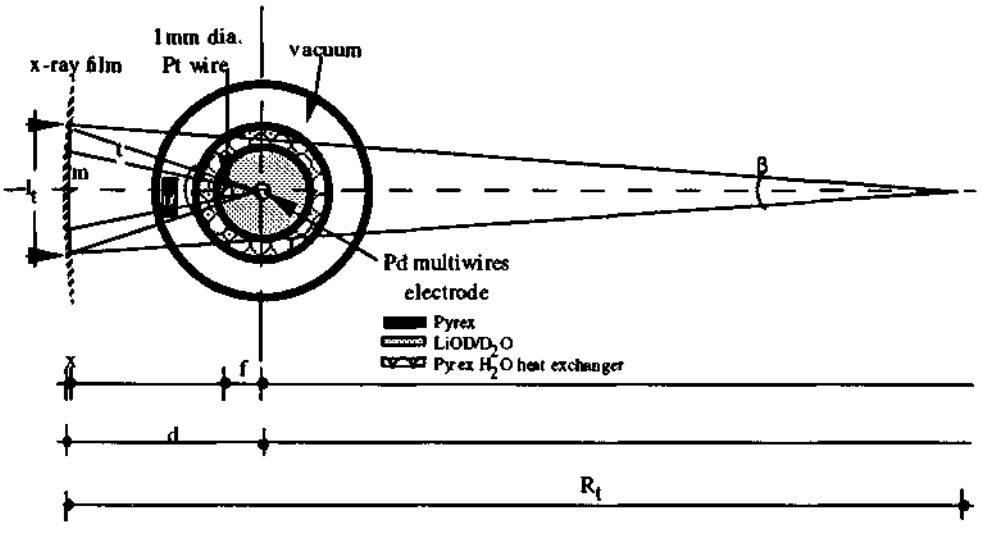

neither with any part of the cell nor with chemicals, therefore any damage of the film producing apparent traces or spots was eliminated. The analysis of the film was carried out by microdensitometer by steps of 600 μm along Z-axis making at each step a scan of X-axis by using a 50 μm slit. To convert the optical density data into exposure units (Roentgen), a calibration was done through known expositions of the same type of film (and using the same developing conditions) to the tungsten K_α radiation filtered by 0.5 mm Al.

2.4 High Resolution Mass Spectrometry (HRMS)

In the gas stream coming out the electrolytic cells

With respect to the previous procedure reported in literature[14], some important improvements were brought to the ^4He determination in the electrolysis gas phase. In the present case, sampling and measurement are carried out on-line and this allows at least two great advantages: to avoid a potential source of contamination by atmospheric ^4He and to increase considerably the number of measurements. All this has been made possible by implementing the experiment with a high resolution quadrupole mass spectrometer (Balzers QMS 421 gas tight crossbeam ion source and analyzer QMA 410) full PC controlled and equipped with some features which allow to automatize several operations such as the on-line sampling. The nominal mass range of QMS in HR mode is 27 amu. The sampling procedure for ^4He is realized after the deuterium removing system[6] has reduced the deuterium content of the gas mixture coming from the cell. A 150 cm^3 SS cylinder (for each cell line), having at both the ends a three-way electrovalve, is in normal position fluxed with the gas mixture and when both the electrovalves are powered for 10 s, the inlet end becomes closed (the stream of the gas mixture is deviated elsewhere to avoid overpressure on the line) and outlet end is connected to SS charcoal trap kept under vacuum and in LN_2. When the electrovalves are again off the cylinder sucks N_2 from a small tank connected to the LN_2 reservoir. When the pressure inside the cylinder becomes higher than the pressure of the line, the line is again connected to the cylinder ready for an other sampling. The gas mixture trapped in the cylinder is let to be adsorbed in the LN_2 charcoal trap until the pressure becomes lower than a preset threshold (typically $5x10^{-2}$ mbar) then the immission of the gas mixture in the QMS chamber is realised. HRMS measurements were carried out in Multiple Ion Detection (MID) mode and the following ionic currents have been generally monitored for the species: $^4He^+$ (4.0026), valley ^4He-D_2 (4.0111), D_2^+ (4.0282), $^{20}Ne^{++}$ (9.996). The pressures in the QMS chamber, in LN_2 trap and in the sampling cylinder were also monitored during each measurement. The software controls the samplings at a given interval of time (typically every 20 min) as well as each related measurement. The mass corresponding to the

valley between ^4He-D_2 is a key parameter for monitoring the complete separation between the two peaks of ^4He and D_2. This always occurs when the deuterium removing system works properly. The presence of relevant quantities of deuterium with respect to ^4He makes impossible its determination. Reliable ^4He measurements can be obtained if the ratio $D_2/^4He$ is lower than ≈3000. The monitoring of $^{20}Ne^+$ was for the first time used in this kind of measurements by us[14]as marker of a possible air contamination. It was also reported[14] that around 20 amu the mass spectra is complicated by the presence of several species which can compromise the use of such a marker. So, the monitoring of double ionized Ne there proposed[14], it is here preferred because, by making use of a MS with lower resolution, $^{20}Ne^{++}$ appears in a mass range without any relevant interference. Several calibrations made before and during the experiment, according to a well-established procedure[14], were done to have the control of the sensitivity, σ, of the QMS (see below). The equation: $Tat = 2.46 \times 10^{-2} c V_s$ holds between the absolute quantity of ^4He atoms in tera atoms (10^{12} atoms) and their concentration in ppb in the gas mixture contained in the sampling volume V_s, given in cm^3, at stp. This allows to give σ in pA/Tat or in pA/ppb. Specific measurements were performed to establish the transport of a ^4He *parcel* along the line by releasing known amounts of air in the cell.

In the Pd electrodes

A home-made device has been realized to detect helium in the bulk of the Pd cathodes by making use of the Thermal Desorption Spectrometry (TDS). The experimental set-up is constituted by a high vacuum pumping system connected to the heating chamber by a gate valve. The heating chamber is connected to the QMS through a gettering line for removing D_2 before the immission in the QMS. The heating element is a vertical cylinder-shaped tantalum foil 75 μm thick in which a graphite crucible is positioned. The samples, as cut sections of the cathodes, are stored in a multiple sample holder driven by an external manipulator. At fixed displacements of the manipulator, each sample is allowed to fall in the crucible. The standard procedure adopted is first to heat the crucible over the m.p. of Pd (1552 °C) under high vacuum pumping then, after having closed the gate valve, to make the sample to fall into the crucible while increasing temperature above 1650 °C, and maintain this temperature for at least 10 min.; finally a rapid cooling follows. At the same time, the evolved gases are allowed to be gettered and, finally, when the pressure in the system decreases below 2×10^{-5} mbar, the QMS is connected and the measure is carried out in MID mode.

3. Results

Figure 3 shows the time pattern of the excess heat power and the absolute quantity of ^4He measured throughout an entire experiment. ^4He is given in tera atoms. The ^4He measurements before the starting of the electrolysis show that, after 200 hrs, 1.7 Tat., corresponding to 0.5 ppb, were still

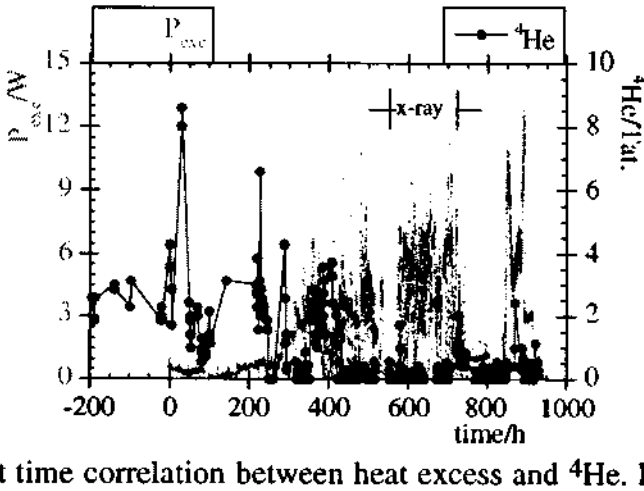

Fig. 3. Excess heat power (left scale) and ^4He (right scale) in an experiment with bundle-type cathode (250 μm dia. wires)

present though ^4He in boiling-off LN_2 is undetectable when measured directly at outlet of the LN_2 reservoir. Since, each component of the line was carefully tested for leaks and all the connections were proved to be safe (SS Swagelock type), we attribute that value to an incomplete washing of the whole line. This is also supported by several measurements made later on in the experiment which did not give any ^4He. At first glance, there is not a direct time correlation between heat excess and ^4He. However, it is important to remind that the ^4He measurement is not performed in continous mode as the heat power excess, therefore, a significative volume of the electrolysis gas mixture is lost without being analyzed. Just to have the

Helium and Heat Correlation

figures, 2.24 m^3 about at stp of gas mixture (mostly N_2, D_2, O_2) passed through the line but only 5.73×10^{-2} m^3 at stp were analyzed in the 382 samplings, the case of fig. 3, 150 cm^3 each. This is less than 2.6 %. Assuming that ^4He is all formed at the surface, it is completely and instantaneously released in the gas phase and the nuclear reaction $d + d = {}^4He + 23.8$ MeV (lattice) holds, we calculated (for space reasons more details will be given elsewhere[24]) the amount of ^4He we have to expect at each sampling of fig. 3 considering the measured heat excess. In figure 4 it is reported this calculation together the excess heat power as in fig. 3. The ratio between the measured and calculated ^4He reported in fig 5 is a parameter to check the energy balance. More specifically, the values of the ratio greater than 1 imply that ^4He detected is of atmospheric nature (in this case, probably, because of incomplete washing). On the other hand, from ~220 hours until to the end of

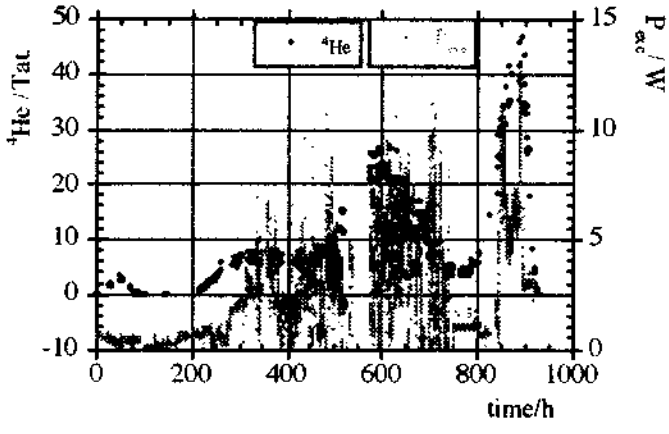

Fig. 4. Calculated ^4He (left scale) and heat power excess (right scale)

the experiment, when the aforementioned ratio is steadily below unity, it is interesting to observe that there are several points definitely greater than zero and fairly close to the energy balance of the process. As for the measurements performed on $^{20}Ne^{++}$ as a marker of contamination these are affected by some uncertainties. Contrarily to the ^4He sensitivity that has been found to be extremely reproducible, 25±3 pA/ppb or 7±1 pA/Tat, during all the experiment, the $^{20}Ne^{++}$ apparent sensitivity was found to be scattered and decreased on time from ~2 to ~0.3 pA/Tat. Moreover the amount of Ne detected has been always at the limit of detectability. The resulting measured ratios He/Ne, in spite of being generally greater than 0.29 (that of the air), are affected by a large error that, conservatively, prevented its use. It must also be kept in mind the findings of our previous experiment where a correlation was found between He and Ne even if the He/Ne ratios were greater than 0.29[14]; in the present experiment the very low range of values observed for the helium makes it difficult to look for the absence of such a correlation. On the other hand, after the experiment, the analysis of ^4He on 9 sections out of 14 of that cathode did not reveal any significative amount of ^4He embedded in the PdD_x lattice over the detection limit of ~2 Tat. Concerning the calorimetric results, they are, respectively, in terms of excess heat and highest ratio P_{exc}/P_{in}, 8.3 MJ and 0.8 as for instance in the case of the cell of fig. 3.

Fig. 5. Ratio between measured and calculated ^4He vs time. The insert is a magnified view in the range from 0 to 1.

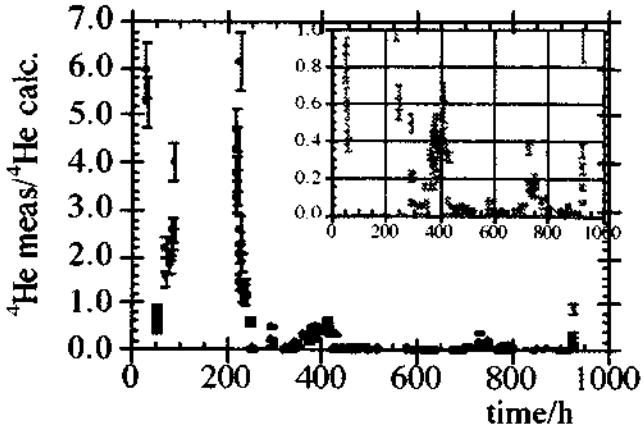

During the experiment, reported in fig. 3, at ≈ 552 hrs since the starting of the electrolysis, a x-ray film was positioned in front to the above cell and an other one in front of the blank cell as reported in fig. 2. After an exposition of a week, the film related to the blank cell did not show any trace whereas the other film showed several spots roughly reproducing the image of the cathode. The intensity, the dimensions and the coordinates of all the spots were measured and reported in figure 6. The spot diameter was found ranging from 0.41 to 2.45 mm. To be sure that an artifact was not occurring, a new film was inserted in the same plastic black bag and exposed to the light of laboratory for some days. The film was not exposed in any point. The plane X,Z is the plane parallel to the film and the vertical axis at X=0 coincides with the Z axis of the cathode, 50 mm far

from the film. In fig. 6 it is clearly visible a quite simmetrical zone, without spots, around the axis at X=0 of the film that could be reasonably attributed to the shadow (m in fig. 2) produced by the 1 mm dia. Pt wire of the anode skeleton (see fig. 2) and parallel to the Z-axis of the cathode. This is supported by the excellent agreement between the shadow width measured (7.00±0.05 mm) and calculated[24] (7.67 mm), assuming the radiation source as point like and localized in the Z-axis of the cathode. If we use the measured value of m to calculate the distance f we obtain f=7.12 mm. There is a deviation of 0.62 mm which is well explained by the deformation of the cathode observed at the end of experiment. The exposition of an x-ray film during an experiment involving energy of a few eV is very difficult to explain in terms of textbook science so that nuclear phenomena have to be necessarily taken into consideration. In the present case, the spot nature further complicates the interpretation of this experimental evidence.

Fig. 6. Microdensitometry of the x-ray film placed parallel to the X,Z plane. Exposure is given in Roentgen (R)

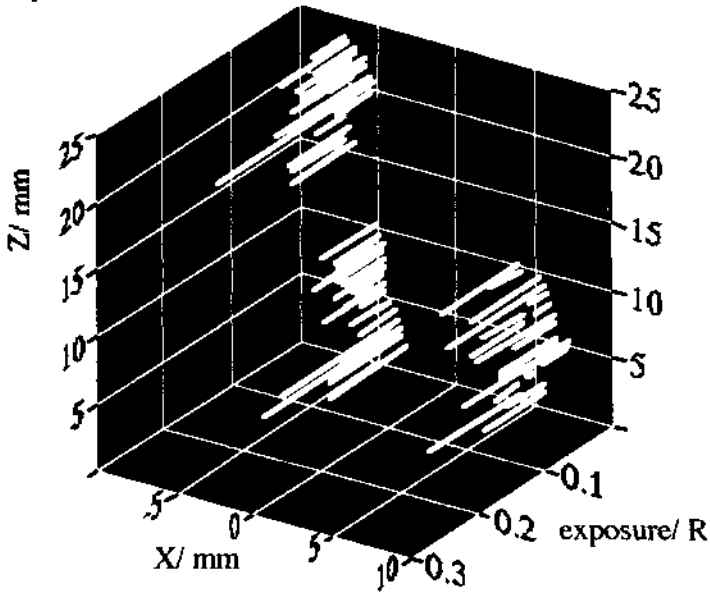

As working hypothesis, consider a whatever primary process which produces directly or indirectly photons sufficiently energetic to cross the cathode and all the materials in between the film. X-ray diffraction can not be reasonably considered because the spot pattern is not a diffraction pattern and, even in the case, the attenuation produced, at the average energy of the K_α lines of Pd (21.61 keV), by all the materials would be total as calculated in figure 7. The question is what is the nature of the source. If the source were coherent, oriented and localized, the pattern found would have its own consistency but we have not enough elements to support this. If the source were a conventional isotropic source some reasonable explanations can be given in terms of physics of radiations. In fact, the first elementary consideration is that the source site is not at the surface of the cathode because a diffuse blakening would be to expected instead of spots. At this point, the shape of the cathode becomes important. In the present case, cathode is bundle shaped and it can be satisfactorily represented by a seven

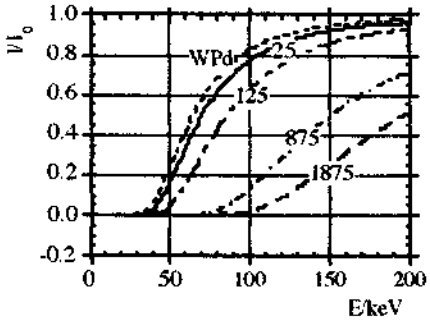

Fig. 7. Attenuation I/I_0 vs photon energy of Pd and materials between cathode and film (WPd=Without Pd) at different thickness (in μm) of Pd crossed.

shells packing as reported below in figure 8. Supposing, for the sake of simplicity, the source in the center of the system, it is easy to verify that the effective path length of the radiation in the cathode depends on the angle of propagation. The minimum and the maximum path lengths, a and b respectively, are expected for a point-like source as in fig. 8. Therefore, the system can be assumed as a system of virtual slits seen as domains in the space where the attenuation, I/I_0, is relatively low according to equation:

$$I/I_0 = \exp[-\sum_i \rho_i(\mu/\rho)_i t_i] = \prod_i \exp[-\rho_i(\mu/\rho)_i t_i] \qquad (3)$$

being ρ, (μ/ρ) and t, respectively, the density, the mass absorption coefficient, which is a function of the photon energy, and the path length of the radiation in a given material i. In the present experimental set-up, the value of eqn. 3 depends only on the photon energy and the position of the source in the cathode, i.e., it depends on the effective path length in Pd. By fig. 7, it is quite evident that at fixed energy the transmission is greatly influenced by that quantity, at least up to 150 keV. As an example, it is shown in fig. 9 the quantity I/I_0 calculated against the angle of propagation of the radiation[24]. The source is supposed to be point-like, localized in the centre of two wires having coordinates (0,0) and

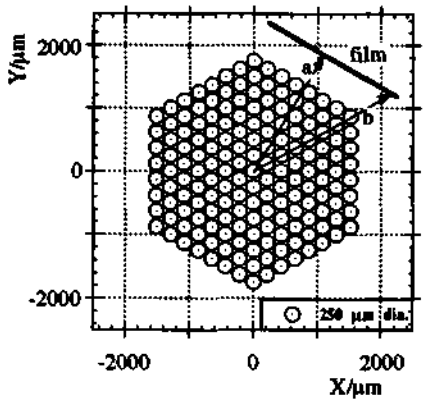

Fig. 8. Representation of the cross-section of an ideal bundle-type cathode with 169 wires of 250 μm dia. The cathodes used were made of 150 wires.

[(433.01,750)-4th shell] and, the emitted radiation, confined, for simplicity, only in a thin slice orthogonal to the z-axis passing in the coordinate origin of fig. 8. It can be shown[24] that more than one peak is found by selecting the source out of the centre of the wire. In principle, the source or sources can be everywhere but we can exclude that they are at the surface of the outermost wires of the bundle because no diffuse blakening of the film was observed. Therefore, sources have to be in the innermost wires. To make an estimation of the energy of the radiation detected the following reasoning can be done:*i.* eqn. 3 is rewritten in the form $I/I_0 = Q exp[-\rho_{Pd}(\mu/\rho)_{Pd} t_{Pd}]$ (4) where $Q = \prod_i exp[-\rho_i(\mu/\rho)_i t_i]$ being the Q term independent on the position of source and practically equal for all the sposts in the film; *ii.* each spot is related to the same type of elementary event and the intensity of a spot depends on the path length the radiation makes through the cathode, i.e., I_0 is always the same; *iii.* the more intense spot is associated to a source closer to the film, i.e., the source is in an outermost wire of the bundle but not in the last shell (see above); *iv.* similarly the weakest spot is related to the source more distant from the film. From the ratio between $\frac{I_{min}/I_0}{I_{max}/I_0}$ and by eqn. 4, the value of the mass absorption coefficient, (μ/ρ), of Pd is obtained.

Fig. 9 Calculated transmission at 90 keV with two different positions of the source in the cathode

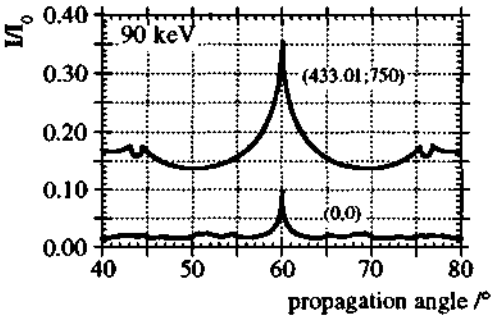

The dependence of (μ/ρ) on photon energy[25] fits very well with the equation $(\mu/\rho)=aE^{-b}$ being a = 310000±5000 and b = 2.676±0.004. Combining the equations, the energy is found by equation:

$$E = \left[\frac{1}{a\rho_{Pd}\left(t_{min} - t_{max}\right)} ln \frac{I_{max}}{I_{min}} \right]^{-1/b}$$ (5). In the above hypotheses, t_{max} and t_{min} have to be selected among the optical paths in Pd which fall in the angle α (fig. 2) correponding to the maximum distance between spots in the film at Z = K (see fig. 6). This angle is 16.32°. The source position has to be selected, respectively, on the surface of any wire in the 6th shell with centre coordinates [0≤X≤1299;750≤Y≤1500] μm and in any wire belonging to the 7th shell with centre coordinates [-1299≤X≤-216.51;-1625≤Y≤-1000] μm. The most appropriate values for t_{max} and t_{min} were found to be, respectively, 250 and 1875 μm. Therefore, E = 89±1 keV was calculated by eqn. 5. The error on E is calculated by taking into account the errors on the fit constant and the experimental error on the intensities which was evaluated less than 2%. At this point, the energy released by this process can be calculated because I_0 can be obtained from eqn. 4. The term Q is represented as function of energy in fig. 7, curve WPd, all the other terms in eqn. 5 are known, I_0 per unity of solid angle is $(4.0\pm0.1)\times10^4$ R. Since the average density of spots in the film is 2750 sterad^{-1}, the total energy on 4π associated to the radiation is 12.0±0.4 kJ (in this calculation, the conversion 1R=87.8 erg has been used). This energy is ≈ 0.5% of the energy measured by calorimetry in the same interval of time during which the film was exposed. Looking at the energy of the K_α lines *vs* the atomic number of the elements, the energy found is close to the energy of the K_α lines of Pb or Bi. Since the chemical analysis did not detect any of them, emission on atomic basis can not be invoked and the nuclear nature of the radiation detected takes place.

Conclusions

The results show a picture with its own internal consistency though the low levels of ^4He do not give the necessary confidence to state definitely that we are dealing with the fusion of deuterons to give ^4He. On the other hand, the contamination is not proved and the energy balance seems quite well satisfied. Moreover, the exposition of the x-ray film is a clear-cut proof (very simple experimental device for which errors of measure and/or of procedure as well as artifacts can not be invoked) that a nuclear phenomenon is at work. We believe that the radiation detected has to be searched among the stable isotopes of Pd or among its impurities having intense nuclear transitions close to the energy found. Work is in progress to check this route.

Acknoweldgements

This work has been supported by the National Research Council (CNR), National Institute of Nuclear Physics (INFN) and University of Rome *La Sapienza.*

References

1. Fleischmann M. and Pons S., *J. Electroanal. Chem.* **1989**, *261*, 301.
2. Noninski V.C. and Noninski C.I., *Fusion Technology* **1993**, *23*, 474.
3. Miles M.H.; Bush B.F. and Stillwell D., *J. Phys. Chem.* **1994**, *98*, 1948.
4. Gozzi D.; Cignini P.L.; Tomellini M.; Frullani S.; Garibaldi F.; Ghio F.; Jodice M. and Urciuoli G. M. , *Fusion Technol.* **1992**, *21*, 60
5. Gozzi D.; Cignini P.L.; Caputo R.; Tomellini M.; Balducci G.; Gigli G.;. Cisbani E.; Frullani S.; Garibaldi F.; Jodice M. and Urciuoli G. M: *Frontiers of Cold Fusion*, Editor H. Ikegami, Frontiers Science Series no.4; Universal Academy Press Inc.: Tokyo **1993**, 155
6. Gozzi D.; Cignini P.L.; Caputo R.; Tomellini M.; Balducci G.; Gigli G.;. Cisbani E.; Frullani S.; Garibaldi F.; Jodice M. and Urciuoli G. M, *J. Electroanal. Chem.* **1995**, *380*, 91.
7. Szpak S.; Mosier-Boss P.A. and Smith J.J., *J. Electroanal. Chem.* **1991**, *302*, 255.
8. Karabut A.B.; Kucherov Ya. R. and Savvatimova I.B., *Phys. Lett.A* **1992**, *170*, 265.
9. Iwamura Y.; Gotoh N.; Itoh T. and Toyoda I., Proc.5th International Conference on Cold Fusion, Monte-Carlo, Monaco, April 9-13, 1995, International Conference on Cold Fusion 5, **1995**, Valbonne, France, p. 197
10. Jones S.E.; Palmer E.P.; Czirr J.B.; Decker D.L.; Jensen G.L.; Thorne J.M.; Taylor S.F. and Rafelski J., *Nature* **1989**, *338*, 737.
11. Bressani T.; Calvo D.; Feliciello A.; Lamberti C.; Iazzi F.; Minetti B.; Cherubini R.; Haque A.M.I. and Ricci R.A., *Nuovo Cimento* **1991**, *104A*, 1413.
12. Takahashi A.; Iida T.; Maekawa F.; Sugimoto H. and Yoshida S., *Fusion Technol.* **1991**, *19*, 380.
13. Okamoto M.; Yoshinaga Y.; Aida M.and Kusunoki T., Proc.4th International Conference on Cold Fusion, Lahaina, Hawaii, Dec. 6-9, 1993,Vol. 2, EPRI TR-104188-V2 **1994** , p.3.
14. Gozzi D.; Cignini P.L.; Caputo R.; Tomellini M.; Balducci G.; Gigli G.;. Cisbani E.; Frullani S.; Garibaldi F.; Jodice M. and Urciuoli G. M, *J. Electroanal. Chem.* **1995**, *380*, 108.
15. Bush B.F.; Lagowski J.J.; Miles M.H. and Ostrom G.S.,*J. Electroanal. Chem.* **1991**, *304*, 271.
16. Yamaguchi E. and Nishioka T. : Frontiers of Cold Fusion, Edited by H. Ikegami, Frontiers Science Series no.4, Universal Academy Press Inc., Tokyo **1993** p.179.
17. Arata Y. and Zhang Y., *Proc. Japan Acad.* **1995**, *71B*, 304.
18. Chien C.C.; Hodko D.; Minevski Z. and Bockris J.O'M., *J. Electroanal. Chem.* **1992**, *338* , 189.
19. Storms E. and Talcott C.L., *Fusion Technol.* **1990**, *17*, 680.
20. Cedzynska K.; Barrowes S.C.; Borgeson H.E.; Knight L.C. and Will F., *Fusion Technol.* **1991**, *20*, 108; **1992**, *22*, 156.
21. Tuggle D.G.; Claytor T.N. and Taylor S.F., Proc.4th International Conference on Cold Fusion, Lahaina, Hawaii, Dec. 6-9, 1993,Vol. 2, EPRI TR-104188-V1 **1994** , p.7.
22. Balej J. and Divisek J. , J. Electroanal. Chem.**1989** *278* 85.
23. *Quantitative Microscopy,* Edited by R.T. DeHoff and F.N. Rhines, Mc Graw Series in Materials Science and Engineering, Mc Graw-Hill Book Co. New York **1968**
24 D. Gozzi et al., paper in preparation
25 J.H. Habbel, Photocross-sections, attenuation coefficient and energy absorption coefficients from 10 keV to 100 GeV, Natl.Stand. Ref. Data, Ser. 29 (1969)